

# EarthMarker: Visual Prompt Learning for Region-level and Point-level Remote Sensing Imagery Comprehension

Wei Zhang<sup>\*</sup>, Miaoxin Cai<sup>\*</sup>, *Graduate Student Member, IEEE*, Tong Zhang, *Graduate Student Member, IEEE*, Jun Li, *Fellow, IEEE*, Yin Zhuang<sup>†</sup> *Member, IEEE*, and Xuerui Mao<sup>‡</sup>

**Abstract**—Recent advances in visual prompting in the natural image area have allowed users to interact with artificial intelligence (AI) tools through various visual marks such as box, point, and free-form shapes. However, due to the significant difference between the natural and remote sensing (RS) images, existing visual prompting models face challenges in RS scenarios. Moreover, RS MLLMs mainly focus on interpreting image-level RS data and only support interaction with language instruction, restricting flexibility applications in the real world. To address those limitations, the first visual prompting model named EarthMarker is proposed, which excels in image-level, region-level, and point-level RS imagery interpretation. Specifically, the visual prompts alongside images and text instruction input into the large language model (LLM), adapt models toward specific predictions and tasks. Subsequently, a sharing visual encoding method is introduced to refine multi-scale image features and visual prompt information uniformly. Furthermore, to endow the EarthMarker with versatile multi-granularity visual perception abilities, the cross-domain phased learning strategy is developed, and the disjoint parameters are optimized in a lightweight manner by leveraging both the natural and RS domain-specific knowledge. In addition, to tackle the lack of RS visual prompting data, a dataset named RSVP featuring multi-modal fine-grained visual prompting instruction is constructed. Extensive experiments are conducted to demonstrate the proposed EarthMarker’s competitive performance, representing a significant advance in multi-granularity RS imagery interpretation under the visual prompting learning framework. Our code and dataset are available at <https://github.com/wivizhang/EarthMarker>.

**Index Terms**—Visual prompting, Remote sensing, Multi-modal large language models (MLLMs).

<sup>\*</sup> Wei Zhang and Miaoxin Cai contributed equally to this work.

<sup>†</sup> Co-corresponding author: Yin Zhuang and Xuerui Mao.

Wei Zhang is with the Advanced Research Institute of Multidisciplinary Sciences, Beijing Institute of Technology, Beijing 100081, China, and also with the School of Mechatronical Engineering, Beijing Institute of Technology, Beijing 100081, China. (e-mail: w.w.zhanger@gmail.com, 3120235339@bit.edu.cn).

Xuerui Mao is with the Advanced Research Institute of Multidisciplinary Sciences, Beijing Institute of Technology, Beijing 100081, China, and with the School of Mechatronical Engineering, Beijing Institute of Technology, Beijing 100081, China, and also with Yangtze Delta Region Academy of Beijing Institute of Technology, Jiaxing 314003, China. (e-mail: maoxuerui@sina.com).

Yin Zhuang, Miaoxin Cai, and Tong Zhang are with the National Key Laboratory of Science and Technology on Space-Born Intelligent Information Processing, Beijing Institute of Technology, Beijing 100081, China. (e-mail: yzhuang@bit.edu.cn, 3120220667@bit.edu.cn, bit\_zhangtong@163.com).

Jun Li is with the School of Computer Science and Hubei Key Laboratory of Intelligent Geo-Information Processing, China University of Geosciences, Wuhan, 430078, China (e-mail: lijuncug@cug.edu.cn).

## I. INTRODUCTION

VISUAL prompting refers to the technique of guiding the visual models to focus on the region of interest and improving their finer-grained interaction performance by providing them with visual marks (e.g., boxes, points, masks) or examples [1]–[3]. Recently, multi-modal large language models (MLLMs) [4], [5] have experienced remarkable advancements in the remote sensing (RS) domain. However, those MLLMs only support language instruction and fail to understand the images in a visual prompting manner. Considering that the high-resolution RS imagery is characterized by scale variation, across categories and tiny objects, fine-grained reasoning is necessary alongside holistic scene interpretation. This is crucial to perform more detailed analyses to make informed decisions in real-world applications [6]. Nevertheless, most existing MLLMs achieve visual-language alignment using image-text pairs, lacking fine-grained referring understanding abilities, such as region-level and point-level. At present, leveraging the visual prompting method to enhance the complex visual reasoning capabilities of MLLMs in RS remains under-explored.

Notably, prompting engineering [7], [8] has been extensively studied in the natural language processing (NLP) community [9] and subsequently spread to the computer vision area. A key example is the Segment Anything (SAM) [10] model, which utilizes multiple visual prompting marks to realize zero-shot segmentation adapted for various new image distributions. However, SAM lacks semantic information, hindering real-world applications. GPT4RoI [11] and Region-Blip [12] have enabled MLLMs to complete region-level visual understanding tasks by training on region-text pairs. Nevertheless, they only support bounding boxes as visual prompts, which lacks flexibility. Osprey [13] excels in pixel-level visual understanding but relies on pre-attached segmentation models, constraining its application range. Additionally, Ferret [14] and SPHINX-V [15] support free-shape visual prompting marks to achieve pixel-level image comprehension. However, all these models are trained on natural scene data, leading to inferior performance when handling the RS imagery.

In the RS field, there are limited works devoted to region-level imagery interpretation. For example, RSVG [16] adopts language prompting to inquire and localize the specific object, but does not involve the visual prompting technique to realize various visual tasks. In addition, inspired by SAM,

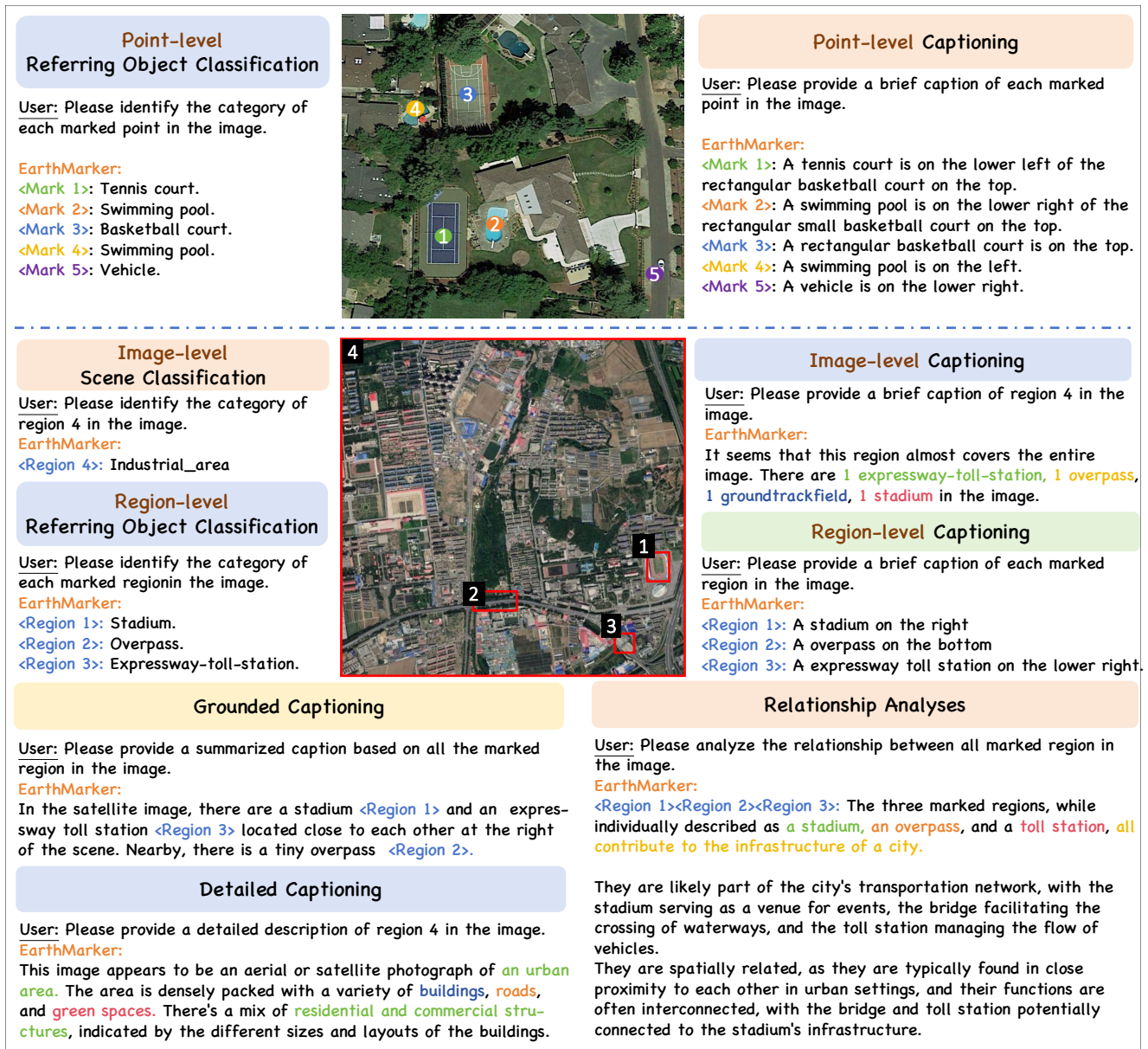


Fig. 1. Examples of multi-granularity (e.g., image-level, region-level, and point-level) RS imagery interpretation by the proposed EarthMarker, which excels in various visual tasks including scene classification, referring object classification, captioning, and relationship analyses.

RSPrompter [17] introduces an automated prompts generation to develop interactive segmentation in RS imagery. Another representative work is EarthGPT [5], which shows the potential of region-level image comprehension by training on visual grounding datasets. However, EarthGPT only supports language interaction without visual prompts, thereby lacking flexibility. These limitations hinder the development of fine-grained spatial understanding and complex reasoning execution in the RS domain. It is clear that the visual prompts learning in the RS domain is still in its infancy.

To bridge this gap, a fine-grained MLLM named EarthMarker is proposed, leveraging visual prompting to extend the capability of MLLMs for region-level and point-level understanding in the RS domain for the first time. Based on the visual prompts learning, as illustrated in Fig. 1, EarthMarker

excels at the multi-granularity interpretation of RS imagery across image, region, and point levels. Moreover, EarthMarker can complete a wide range of RS visual reasoning tasks, including scene classification, referring object classification, captioning, inter-relationship analyses, etc. Concretely, the visual prompts, i.e., bounding boxes and points, along with the RS images and the text instructions are provided as input to the LLM. Notably, the visual prompting marks are utilized to isolate specific areas and guide the model to interpret regional content in the entire RS image. Considering that the RS imagery is gathered from an overhead perspective by satellites, associated with large-scale variations and cluttered backgrounds, multi-resolution image input processing is necessary. Subsequently, unlike most existing nature scene visual prompting works, which routinely set different visual

encoders and visual prompts encoders. In our method, a sharing visual encoding method is developed. Specifically, the visual prompt is processed to RGB images analogously, which shares the same visual encoder with the inputted image. This strategy is beneficial for consistent feature extraction and understanding the relationship between visual prompts regions and the holistic image, enhancing the performance of the model under visual prompts learning.

In order to enhance the *visual prompts-image-text* alignment and to equip the EarthMarker with versatile multi-granularity visual comprehension abilities, the cross-domain phased learning strategy is proposed. In the first stage for multi-domain image-text alignment, EarthMarker is trained on the existing nature scene and RS caption data to obtain general image understanding and enhance the modeling of conceptual diversity. Subsequently, the model is further trained on the nature domain referring data to achieve spatial perception in images, beneficial for subsequent developing referring comprehension ability in the RS domain. Lastly, in the RS visual prompting tuning stage, leveraging RS region-text and point-text instruction data, the proposed EarthMarker is equipped with point-level and region-level RS imagery interpretation capability. Notably, the phased training leverages the natural domain generalized knowledge and the RS domain expert knowledge for developing RS visual prompting MLLM. The multi-domain joint training is advantageous for enhancing the deep interpretation of fine-grained RS imagery and improving open-vocabulary reasoning capabilities. In addition, the updatable parameters of the model are disjoint, preventing interference between understanding images at different granularity and the capability to follow the visual prompt instruction.

Another challenge lies in the datasets, e.g., existing visual prompting datasets [13], [14] are restricted to the natural scene, lacking RS semantics. It has become indispensable to construct a visual prompting dataset tailored to the RS domain for developing fine-grained MLLM. To this end, a RS visual prompting dataset named RSVP-3M, featuring large-scale fine-grained instruction-following, is developed. In particular, diverse publicly available RS data are transformed and re-annotated into uniform conversation formats. Furthermore, part of the more high-quality caption data is generated from GPT-4V [18]. Those captions are uniquely tailored with the distinctive characteristics of each RS imagery, thereby enhancing the richness and diversity of data. Through the data conversion and re-annotation from existing datasets and GPT-4V, over 3M image-point-text and image-region-text pairings are constructed, covering a wide geographic distribution and multiple types of ground targets.

Extensive experiments are conducted on multi-type RS datasets to evaluate the performance of EarthMarker which is demonstrated to be superior to state-of-the-art (SOTA) specialist models, MLLMs, and visual prompting models in various RS visual tasks at different granularity. Specifically, for the zero-shot scene classification task, EarthMarker shows a significant improvement compared with other existing MLLMs. Notably, for referring object classification, EarthMarker achieves a Semantic Similarity (SS) score of 98.37 % using bounding boxes as visual prompts and 95.96 % using

point prompts on DIOR-RSVG dataset [19]. Furthermore, for image and region captioning tasks, EarthMarker also far exceeds other MLLMs and visual prompting models. In summary, the experimental results demonstrate that EarthMarker exhibits exceptional performance across a variety of multi-granularity RS image comprehension tasks and excellent zero-shot reasoning capability.

Our contributions can be summarized as follows.

- *The First RS Visual Prompting Dataset, RSVP.* A large-scale RS regional instruction dataset named RSVP-3M, containing over 3M image-point-text and image-region-text pairings, is constructed. The construction of RSVP-3M facilitates fine-grained RS imagery interpretation, laying the foundation for the development of visual prompting in the RS domain.
- *The First RS Visual Prompting MLLM, EarthMarker.* Leveraging our newly constructed RSVP, the visual prompting MLLM named EarthMarker is proposed. EarthMarker can interpret RS imagery in the multi-turn conversation at different granularity, including image, region, and point levels, significantly catering to the fine-grained interpretation needs for RS imagery.
- *The First RS Visual Prompt Learning Framework.* A universal region and point-level visual prompting data annotation method is developed. Subsequently, a sharing visual encoding mechanism is proposed, which adapts visual prompts to match the dimensions of the input image, thereby both of them undergo uniform processing by the same visual encoder. This mechanism comprehensively enhances the interplay among visual prompts, holistic images, and text instructions. Furthermore, the cross-domain phased learning strategy is designed, and the disjoint parameters are optimized in a lightweight manner by leveraging the multi-domain data, endowing EarthMarker with spatial perception and visual prompting following capabilities.
- *Superior Performance on Multi-granularity RS Visual Tasks.* Extensive experiments are conducted to demonstrate EarthMarker’s competitive performance in multi-granularity RS visual interpretation tasks, compared with the SOTA specialist models, MLLMs, and visual prompting models. The tasks evaluated include scene classification, referring object classification, captioning, and inter-relationship analyses. Therefore, EarthMarker successfully explores the adaptation of the visual prompt learning in the RS domain, improving the performance of MLLM and representing a significant step in fine-grained RS imagery interpretation.

## II. RELATED WORK

### A. Multi-modal Large Language Models (MLLMs)

Recently, the advancement of large language models (LLMs) has significantly fueled the revolution and innovation in the natural language processing (NLP) field. The representative works including closed-source GPT series [11], [20] and open-source LLaMA series [21], [22] have achieved powerful

generalizable language processing and reasoning ability. Inspired by LLM and by further injecting visual signals, MLLMs are developed for visual-language mutual comprehension and various visual tasks. For example, VisualGPT [23], BLIP [24] and Flamingo [25] show strong multi-modal reasoning potential after aligning LLMs with visual modality. Notably, LLAMA-Adapter V2 [26] and SPHINX [27] adopt zero-shot attention mechanism and linear projection layers tuning to mix LLM with visual signal. Those nature scene MLLMs laid the foundation for the extension to the remote sensing (RS) domain.

Some pioneer RS MLLMs have emerged, and related studies such as EarthGPT [5], Geochat [4], and SkyEyeGPT [28] have enabled MLLMs to interpret RS imagery. Among them, Geochat is the first MLLM targeting solving multiple tasks on optical RS images. Furthermore, EarthGPT has proposed a more universal MLLM that can deal with multi-source RS imagery and a wide range of RS visual tasks. There is no doubt that those models facilitate the development of MLLMs in the RS-specific domain. However, those models complete visual interpretation only through human-like language interactions, but cannot generate responses through visual prompts. Apparently, existing RS MLLMs mainly focus on image-level and visual grounding, but are incapable of referring comprehension. Therefore, this paper aims to enhance the MLLMs for referring fine-grained understanding of vision.

### B. Prompt Engineering

Prompt engineering is an emerging research direction in NLP [20]. Representation works contain AutoPrompt [7] and CoOp [8], which are designed to automate prompt template generation for language and vision-language models, instead of manual crafting. Additionally, language prompting has been applied for developing open-vocabulary detection models such as DetPro [29] and Promptdet [30]. Compared with the extensively developed language prompting technique, visual prompting also needs more exploration. A major development is the Segment Anything (SAM) [10] model, which supports multiple segmentation prompts to enhance the zero-shot performance. Due to the lack of semantic labels in SAM, the Semantic-SAM [31] is proposed to realize multi-level semantics analysis and prediction. Notably, GPT4RoI [11] uses spatial boxes, and combines language and region-of-interest for input, enabling regional recognition. Colorful Prompting Tuning (CPT) [32] uses color-based markers to improve the performance of pre-trained vision-language models. The aforementioned models are trained on nature scene datasets. Note that Osprey [13] incorporates fine-grained mask regions into language instruction, achieving pixel-level visual understanding. Other visual prompting works including RegionBlip [12], Kosmos-2 [33], Shikra [34], and Ferret [14], also have shown promising results in region-based image understanding by leveraging visual prompting techniques. Additionally, the study entitled ‘‘Visual Prompting via Image Inpainting’’ [1] shows that various vision tasks can be accomplished well by giving desired task examples.

There are pioneering studies in the RS domain on region-level image understanding. For example, RSVG [16] can

provide the referred object’s bounding box based on images and natural language expression. Moreover, EarthGPT [5] also has the visual grounding ability, and it is capable of providing captions for specific areas within images. Inspired by prompt learning, RSPrompter [17] designs an automated approach to generate appropriate prompts for SAM input, facilitating RS imagery segmentation. However, RSVG adopts language prompting but without visual prompting, whilst RSPrompter is only tailored to the segmentation task. Apparently, there is no unified visual prompting framework designed for the RS domain to further improve the performance of MLLMs. Those limitations hamper the development of more complex and fine-grained RS imagery understanding, therefore this paper focuses on filling this gap.

## III. METHODOLOGY

We first overview the overall model architecture in Section III-A. Subsequently, the three-phase continuous training strategy of the proposed EarthMarker is detailed in Section III-B.

### A. Model Architecture

One challenge in the RS domain is the absence of a visual prompts learning framework to endow MLLMs with fine-grained image understanding capabilities, blocking more complex reasoning. To address this challenge, EarthMarker is proposed, utilizing visual prompting for multi-granularity RS imagery comprehension. As illustrated in Fig. 2, EarthMarker contains four core components: a sharing visual encoding mechanism, a modality-align projection layer, a text tokenizer module, and a LLM decoder. These components work together to deal with multi-modal information, such as text instruction, images, and diverse visual prompting marks including bounding boxes and points, allowing LLM to generate accurate text responses. Each part is introduced as follows in detail.

In particular, the images and corresponding visual prompts share a visual encoding mechanism for feature sharing, enabling the visual encoders to better understand and associate the relationship between images and visual prompts. Specifically, the Mixture of Visual Experts (MoV) [35] is designed to encode the visual information. The MoV incorporates two visual encoders, DINOv2-ViT L/14 [36] and CLIP-ConvNeXt [37], which are pre-trained on distinct network architectures (ViT and CNN), thus offering complementary visual semantics. To refine the robust multi-scale visual features, the input images  $I$  are downsampled to different resolutions denoted as  $I^i$  and then respectively fed into the MoV module to encode. Leveraging the strengths of various visual backbones, visual perception is enhanced and key details in images are refined. Subsequently, the encoded visual features are transformed to the same dimension and concatenated channel-wisely to obtain the integrated multi-scale feature maps represented as  $V_{\text{img}}$ . This process can be formulated as

$$V_{\text{img}} = \text{Concat}(\text{MoV}(I^i)), \quad i = 1, 2, \dots, N. \quad (1)$$

Notably, a key step to the encoder-sharing mechanism is the ‘‘Visual Prompt as Images’’. Especially, the dimension ( $H \times W \times 1$ ) of the visual prompts is processed to the same

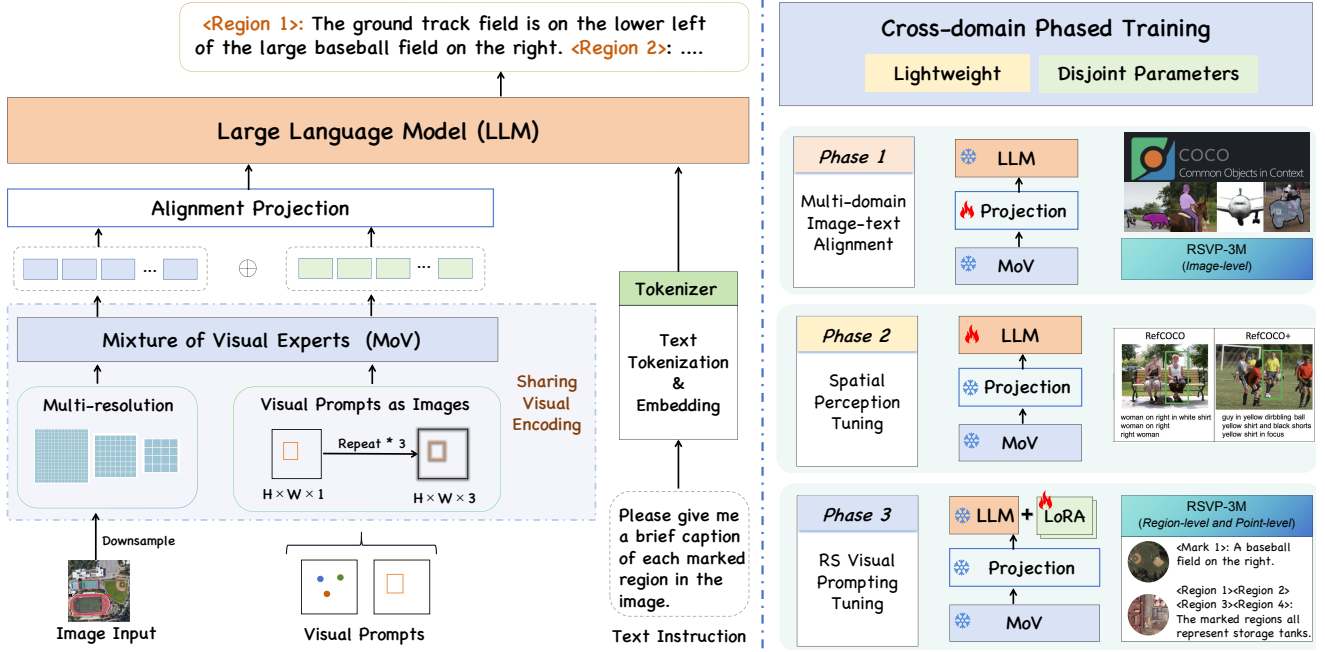


Fig. 2. Left: Overall model architecture of the proposed EarthMarker. Right: Cross-domain Phased Training method.

dimension ( $H \times W \times 3$ ) with the images. Then, the transformed visual prompts  $P$  also can be fed into MoV together with the images, the encoded visual prompts expressed as  $V_{\text{prompt}}$ . Similarly, this process is written as

$$V_{\text{prompt}} = \text{MoV}(P). \quad (2)$$

Subsequently, the modality alignment projection layer  $\Phi$  transforms the visual tokens into the language semantic space. Meanwhile, the text instructions are processed by the tokenizer module, which handles text tokenization and embedding, converting them into text embeddings  $X_{\text{instruct}}$ . After obtaining the projected image tokens, visual prompts tokens, and text instructions embeddings, they are integrated into an entire multi-modal input sequence. LLM decoder takes the multi-modal inputs and generates the response sequence  $Y$ , which can be formulated as

$$Y = \text{LLM}(\Phi(V_{\text{img}}), \Phi(V_{\text{prompt}}), X_{\text{instruct}}). \quad (3)$$

It should be noted that we employ Llama 2, a transformer-based decoder-only LLM, as the LLM decoder.

### B. Cross-domain Phased Training

To realize the fundamental image-level understanding, spatial perception, and region/point-level RS data interpretation ability, the cross-domain phased training method is designed. The entire training process is divided into three phases including multi-domain image-text alignment, spatial perception tuning, and RS visual prompting tuning stage. Throughout the training, we keep lightweight training and avoid expensive full-parameters tuning. Furthermore, the disjoint parameters strategy is proposed, namely, the updated parameters of each stage are different. This strategy is conducive to the step-by-step solid understanding of images, and naturally solves the

interference between image-text understanding, visual prompting comprehension, and fine-grained instruction-following.

**Multi-domain Image-text Alignment.** The first phase employs a multi-domain image-text alignment strategy. In this stage, both natural and RS domain image-level data are leveraged for pre-training to bring visual and text knowledge into alignment within a high-dimensional feature space. This strategy enables EarthMarker to deeply understand the holistic semantics of images. Specifically, we utilize the natural scene caption dataset COCO Caption [38], alongside the RS image caption and scene classification subset from the newly constructed RSVP. During this training phase, multi-scale visual features and language representations are integrated into the LLM to develop image-level comprehension capabilities. The MoV module is kept frozen throughout the training, so as to concentrate on refining robust visual features. Only the alignment projection layer, which acts as the visual-language connector, undergoes parameter updates to enhance the multi-modal capabilities of the proposed EarthMarker and ensure seamless integration of visual and textual information.

**Spatial Perception Tuning.** In the previous step, EarthMarker achieved image-level comprehension capability. In this step, to acquire spatial perception and object-level comprehension, the nature scene publicly available datasets, RefCOCO [39] and RefCOCO+ [40] are transformed into the instruction-following format. Throughout the training, the attention layers of LLM are unfrozen for aligning spatial region features with language embeddings. Specifically, LLM's key module self-attention head is composed of key  $K$ , query  $Q$ , and the value  $V$ , which are transformed by several linear layers. The  $l$ -th implementation equations can be expressed as follows

$$Q_l(X) = W_l^q X + b_l^q, \quad (4)$$

$$K_l(X) = W_l^k X + b_l^k, \quad (5)$$

$$V_l(X) = W_l^v X + b_l^v, \quad (6)$$

where  $X$  represents multi-modal input. The parameters  $W_q$ ,  $W_k$ ,  $W_v$ ,  $b_q$ ,  $b_k$ , and  $b_v$  are updated during the training. Then, the  $l$ -th single attention scores of Q and K are calculated as

$$\text{Attn}_l(Q_l, K_l, V_l) = V_l \times \text{Softmax}\left(\frac{Q_l K_l^T}{\sqrt{d_K}}\right), \quad (7)$$

where  $\sqrt{d_K}$  is the dimensionality of the keys. In addition, the other modules are kept frozen.

**RS Visual Prompting Tuning.** The last stage focuses on accurately following user instructions and achieving complex region-level and point-level visual reasoning tasks. The MoV, alignment projection, and LLM are fixed. The LoRA method is adopted for tuning. We load the weights trained in the previous phase and continue training EarthMarker on RSVP-3M region-text and point-text pairings, which contain the fine-grained referring object classification and referring brief caption data. Specifically, several learnable low-rank adapter matrices  $\Delta W_{h,l}^o$ ,  $\Delta W_{h,l}^v$ ,  $\Delta W_{h,l}^q$ , and  $\Delta W_{h,l}^k$  are inserted into Transformer layers of LLM. The  $H$  is the number of attention heads. The adapted multi-head attention is denoted as  $\text{MultiAttn}_l^*$ , thus the output of the  $l$ -th adapted Transformer attention is formulated as

$$\text{MultiAttn}_l^* = \sum_{h=1}^H (O_{h,l} + \Delta W_{h,l}^o) \times (V_{h,l} + \Delta W_{h,l}^v) \quad (8)$$

$$\times \text{Softmax}\left(\frac{(Q_{h,l} + \Delta W_{h,l}^q)(K_{h,l}^T + \Delta W_{h,l}^k)}{\sqrt{d_K}}\right).$$

In conclusion, the cross-domain phased training endows EarthMarker with various granular (e.g., image-level, point-level, and region-level) multimodal instruction capabilities in the RS domain. In the first multi-domain image-text alignment stage, the LLM is efficiently converted into an MLLM, which is capable of image-level understanding. Subsequently, by utilizing the nature scene referring datasets, EarthMarker is equipped with the fundamental spatial perception of images. This is beneficial for subsequent developments of referring ability in the RS domain. Furthermore, by leveraging the RS visual prompting datasets RSVP-3M, EarthMarker is endowed with image understanding at both the region level and point level. Notably, different field’s datasets are adopted for training, and enhancing open-vocabulary reasoning ability. It should be emphasized that during the whole training, our updatable parameters are disjoint, preventing interference between understanding images at different granularity and the capability to follow visual prompts.

#### IV. RS VISUAL PROMPTING DATASET CONSTRUCTION

In this section, a visual prompting dataset named RSVP-3M is presented. RSVP-3M is the first visual prompting instruction dataset in the RS field, designed to advance image-level and fine-grained point-level, region-level RS MLLMs. Specifically, RSVP-3M contains over 3 million multimodal dialogue data with visual prompting marks. Those multi-granularity visual

prompting data are restructured and cleaned from existing publicly available RS datasets. Furthermore, the GPT-4V [18] is employed for automatic annotation to construct a high-quality complex visual reasoning dataset [15]. A detailed explanation of the construction of the RSVP-3M dataset is introduced as follows.

##### A. Data Conversion and Annotation from Public RS Datasets

A part data of the dataset RSVP-3M is constructed by restructuring and relabeling existing RS datasets. A range of visual task types is covered, containing image classification, instance segmentation, object detection, image caption, and region caption, see Tab. I. The image-level, region-level, and point-level data are derived from different RS datasets. Firstly, image-level visual prompting data is converted from image classification and captioning datasets. For the two type datasets, image-level visual instructions are used, with the bounding box  $[0, 0, \text{width}, \text{height}]$  serving as the visual prompt to obtain the image’s category or brief caption. Subsequently, the region-level data is based on object detection datasets. The ground truth bounding boxes are used as visual prompts to guide the model to identify the object-level or region-level categories accurately. Additionally, the point-level data is transformed from segmentation datasets. For instance segmentation, the representative points extracted from masks corresponding to instances are used as point-level visual prompts. For semantic segmentation, each image is divided into  $32 \times 32$  patches, and the points are randomly sampled within each patch as the visual prompts, with the category retrieved from the corresponding segmentation map.

In RSVP-3M, each data item consists of visual prompts, user instructions, and image. The visual prompts in the user instructions or model answers are expressed as  $\langle \text{Mark } i \rangle$  or  $\langle \text{Region } i \rangle$ . For the point-level data, for example, the user instruction which guides referring object classification is “Please identify the category of each marked point in the image”. The answer format is “ $\langle \text{Mark } 1 \rangle$ : Label 1\n  $\langle \text{Mark } 2 \rangle$ : Label 2\n ..., ‘points’:  $[x_1, y_1], [x_2, y_2], \dots$ ”. In addition, for the region-level data, take the scene of the airport as an example. The user instruction for airport region captioning is “Please provide the brief caption of each marked region in the image, and the corresponding answer format generated by the model is “ $\langle \text{Region } 1 \rangle$ : A big airplane on the left\n  $\langle \text{Region } 2 \rangle$ : A small vehicle on the top\n ..., ‘bbox’:  $[x_1, y_1, x_2, y_2], \dots$ ”. The data structures of other visual tasks are similar to those explained above. Through the transformation and re-annotation based on public datasets, the visual prompting dataset RSVP-3M is effectively developed, featuring image-point-text and image-region-text pairings.

##### B. GPT4V-assisted Visual Prompting Data Generation

The aforementioned public datasets only provide simple classification information and brief captions, which are insufficient for intelligent interpretation of complex RS imagery. To mitigate the limitation and develop a more detailed and explicit RS visual prompting dataset, the language prompts

for GPT-4V are carefully crafted for generating data featuring various complex visual reasoning. The complex fine-grained visual tasks involve detailed image captioning, inter-relationship analysis, and grounding captioning. We adopt the Set-of-Marks [64] (SoM) prompting, which can effectively unleash the extraordinary visual grounding ability of GPT-4V, to obtain comprehensive and unique characteristics from the RS imagery.

The data generated using GPT-4V not only compensates for the lack of information in brief captions but also provides

detailed descriptions that reveal the spatial and semantic relationships between different regions in the image. For example, in aerial imagery, it is feasible to identify the general category of the image and provide a simple description. Additionally, detailed descriptions, such as the spatial layout of tennis courts, basketball courts, playgrounds, the relationships among these areas, and the activities of people on the playground, can be conducted. The RSVP-3M dataset, supplemented by public datasets and data generated by GPT-4V, covers a wide range of fine-grained visual reasoning tasks, enhancing the richness and diversity of the data.

TABLE I  
DETAILS ON THE TRAINING SAMPLES USED FOR THE RSVP.

Tasks	Raw Data	Samples
Image Captioning	NWPU-Captions [41]	169,981
	RSITMD [42]	24,387
	Sydney-Captions [43]	2,837
Region Captioning	DIOR-RSVG [19]	31,491
Scene Classification	NWPU-RESISC45 [44]	94,500
	OPTIMAL 31 [45]	3,720
	RSD46 [46]	350,685
	WHU-RS19 [47]	3,015
Referring Object Classification (Box)	DOTA V2 [48]	99,774
	FAR1M [49]	17,074
	NWPUVHR10 [50]	1,888
	RSOD [46]	1,465
	UCAS-AOD [51]	3,203
	VisDrone [52]	128,531
	MAR20 [53]	2,096
	DOSR [54]	1,127
	LEVIR [55]	4,633
	HRSC2016 [56]	2,171
	HRRSD [57]	12,519
Referring Object Classification (Point)	Vaihingen [58]	45,104
	Potsdam [58]	504,139
	Hi-UCD [59]	125,908
	NWPUVHR10 [50]	956
	isAID [60]	294,355
Relationship Analyses	UAVid [61]	1,167,543
	SOTA [62]	171,583
	FAST [62]	263,056
	WHU [63]	33,022
	HRRSD [57]	11,602
	RSOD [46]	934
	NWPUVHR10 [50]	1,950
	LEVIR [55]	3,956
Grounded Captioning	UUCAS-AOD [51]	2,892
	DIOR-RSVG [19]	15,274
	DIOR-RSVG [19]	15,274
	GeoChat [4]	35,264
	NWPUVHR10 [50]	975

## V. EXPERIMENTS

In this section, we present extensive experiments to validate the superior performance of EarthMarker. In Section V-A, we introduce the implementation details. Subsequently, we conduct qualitative and quantitative analyses to provide a holistic view of EarthMarker’s performance from Sections V-B to V-E.

### A. Implementation Details

The proposed EarthMarker adopts the cross-domain phased training strategy, and the parameters updated vary at different stages. In general, we train an off-the-shelf 13B language model Llama 2 and the visual encoder MoV is kept frozen during the training. In the first multi-domain image-text alignment stage, only the alignment projection layer is updated. Then, in the spatial perception tuning phase, only the attention layers of LLM are unfrozen. Furthermore, the trainable LoRA metrics are introduced in the last RS visual prompting tuning stage. We utilized AdamW optimizer [65] with weight decay = 0 and betas = (0.9, 0.95), the learning rate is set to 2e-5, and the total training stages are conducted on 8 NVIDIA A100 GPUs. For model evaluation, we select diverse multi-granularity visual tasks to assess the performance of EarthMarker. Image-level tasks include scene classification and image captioning, while region-level tasks contain referring object classification, region captioning, and relationship analyses.

TABLE II  
ZERO-SHOT COMPARISON RESULTS BETWEEN EARTHMARKER AND OTHER MLLMs ON UCmerced AND AID.

Methods	Publication Year	UCmerced	AID
Qwen-VL-Chat [66]	Arxiv 2023	62.90	52.60
MiniGPTV2 [67]	Arxiv 2023	4.76	12.90
LLaVa-1.5 [68]	NeurIPS 2023	68.00	51.00
Sphinx [27]	Arxiv 2023	62.76	58.20
GeoChat [69]	CVPR 2024	84.43	72.03
<b>EarthMarker(Ours)</b>		<b>86.52</b>	<b>77.97</b>

### B. Scene Classification

For scene classification tasks, we use the AID [74] and UCmerced [75] datasets for evaluation. AID is a large-scale

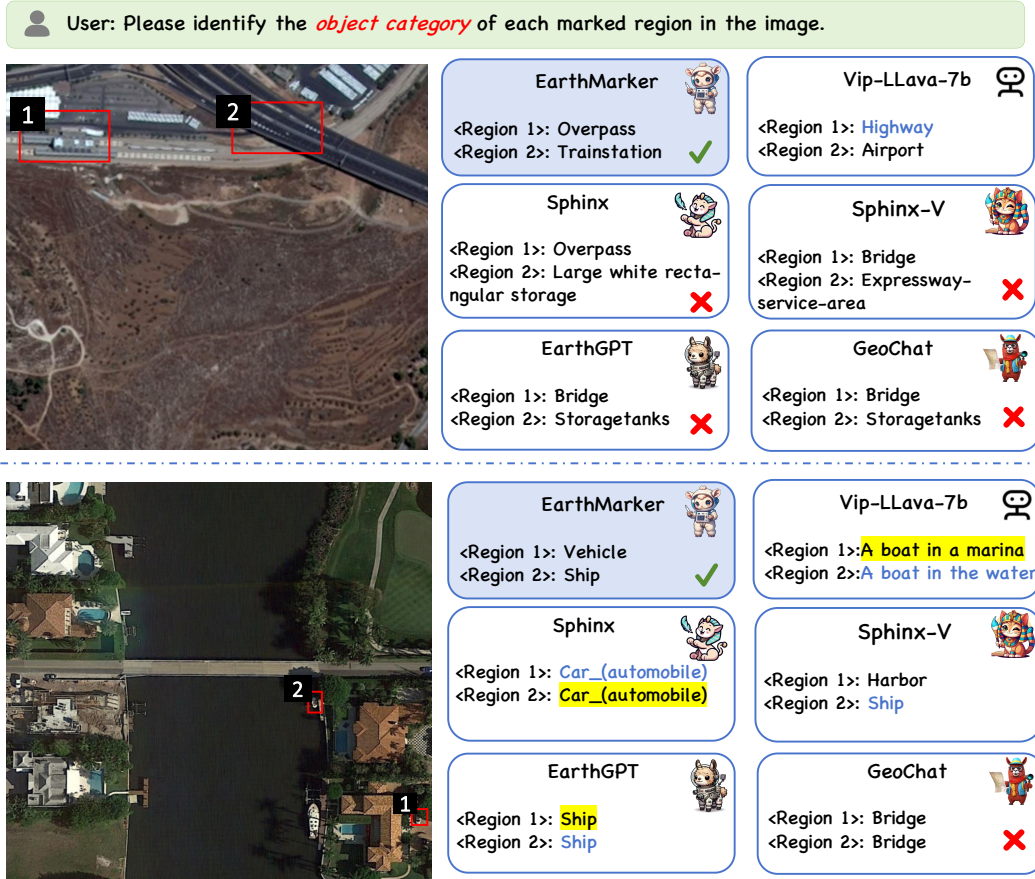


Fig. 3. The Referring object classification results on RS images demonstrate superior region-level RS visual understanding capability of EarthMarker compared to other MLLMs and visual prompting models (The symbol  $\checkmark$  indicates consistency with the ground truth, the symbol  $\times$  represents all incorrect answers, the yellow highlights denote errors, and the blue text represents relatively correct responses).

TABLE III  
SUPERVISED COMPARISON RESULTS ON NWPU-CAPTIONS DATASET BETWEEN EXPERT MODELS AND OUR EARTHMARKER.

Methods	Publication Year	BLEU1	BLEU2	BLEU3	BLEU4	METEOR	ROUGE-L	CIDEr(0-5)	SPICE
<b>Expert Models</b>									
CSMLF [70]	GRSL 2019	77.0	64.9	53.2	47.1	32.0	57.8	106.5	26.5
Qu, et. al [43]	CITS 2016	72.5	60.3	51.8	45.5	33.6	59.1	117.9	27.6
Attention(soft) [71]	TGRS 2017	73.1	60.9	52.5	46.2	33.9	59.9	113.6	<b>28.5</b>
Attention(hard) [71]	TGRS 2017	73.3	61.0	52.7	46.4	34.0	60.0	110.3	28.4
FC-Att [72]	TGRS 2019	73.6	61.5	53.2	46.9	33.8	60.0	123.1	28.3
SM-Att [72]	TGRS 2019	73.9	61.7	53.2	46.8	33.0	59.3	123.6	27.6
MLCA-Net [73]	TGRS 2022	74.5	62.4	54.1	47.8	33.7	60.1	126.4	<b>28.5</b>
<b>Visual Prompting Model</b>									
<b>EarthMarker(Ours)</b>		<b>84.4</b>	<b>73.1</b>	<b>62.9</b>	<b>54.3</b>	<b>37.5</b>	<b>70.0</b>	<b>162.9</b>	26.8

aerial dataset collected from Google Earth, containing 30 categories. Following the setting of GeoChat, we use a 20% split of the AID dataset for testing. The UCmerced dataset consists of 21 categories for scene classification. Following the setting of GeoChat, the entire UCmerced dataset is adopted as a zero-shot test set.

We prompt the model with an image-level box  $[0, 0, \text{width}, \text{height}]$  to represent the entire image. The text instruction is “Please identify the object category of each

marked region in the image”. We calculate the zero-shot accuracy on the AID and UCmerced dataset. EarthMarker significantly outperforms other VLMs, with an accuracy of 86.52% on UCmerced and 77.97% on AID, as presented in Tab. II. In comparison, LLaVa-1.5 and Sphinx, due to the lack of RS domain knowledge, are inferior to the RS MLLM GeoChat and our EarthMarker. Compared to GeoChat, our EarthMarker achieved an accuracy improvement of 5.94% on AID and 2.09% on UCmerced. Owing to the multi-domain



TABLE IV  
COMPARISON RESULTS BETWEEN EARTHMARKER AND OTHER MLLMS, VISUAL PROMPTING MODELS ON THE TEST SET OF DIOR-RSVG IN REGION CAPTIONING TASK.

Method	Publication Year	Formats	BLEU-1	BLEU-2	BLEU-3	BLEU-4	METEOR	ROUGE	CIDER	SPICE
<b>MLLM</b>										
Qwen-VL-Chat [69]	Arxiv 2023	Coor	20.66	9.55	4.90	1.96	8.35	20.93	29.18	9.55
GeoChat [66]	CVPR 2024	Coor	20.86	9.63	5.43	3.25	12.94	26.98	30.92	24.97
Sphinx [27]	Arxiv 2023	Coor	43.32	33.58	27.58	22.81	21.70	47.81	235.07	38.12
EarthGPT [5]	TGRS 2024	Coor	49.73	39.24	32.50	26.79	24.09	47.87	232.79	38.29
<b>Visual Prompting Model</b>										
Sphinx-V [15]	Arxiv 2024	Box	45.19	34.83	28.59	23.64	24.34	50.54	235.09	43.53
Vip-LLava-7b [76]	CVPR 2024	Box	21.03	11.26	6.37	3.25	9.59	23.50	30.95	12.44
Vip-LLava-13b [76]	CVPR 2024	Box	21.68	11.17	6.23	3.38	9.18	23.22	28.58	10.68
GLaMM [76]	CVPR 2024	Box	23.30	14.18	8.78	5.15	11.24	30.36	64.08	17.99
<b>EarthMarker(Ours)</b>		Point	<b>57.45</b>	<b>49.23</b>	<b>43.88</b>	<b>39.46</b>	<b>32.26</b>	<b>61.51</b>	<b>400.76</b>	<b>61.03</b>
<b>EarthMarker(Ours)</b>		Box	<b>57.14</b>	<b>48.60</b>	<b>43.06</b>	<b>38.59</b>	<b>31.97</b>	<b>60.46</b>	<b>379.25</b>	<b>59.87</b>

TABLE V  
COMPARISON RESULTS BETWEEN EARTHMARKER AND OTHER MLLMS, VISUAL PROMPTING MODELS ON THE TEST SET OF DIOR-RSVG.

Methods	Publication Year	Formats	SS	SIOU
<b>MLLMs</b>				
GeoChat [69]	CVPR 2024	Coor	79.59	68.80
Sphinx [27]	Arxiv 2023	Coor	93.72	89.37
EarthGPT [5]	TGRS 2024	Coor	94.64	90.16
<b>Visual Prompting Models</b>				
Sphinx-V [15]	Arxiv 2024	Box	89.07	81.62
Vip-LLava-7b [76]	CVPR 2024	Box	72.56	55.94
Vip-LLava-13b [76]	CVPR 2024	Box	74.51	60.53
<b>EarthMarker(Ours)</b>		Point	<b>95.96</b>	<b>93.49</b>
<b>EarthMarker(Ours)</b>		Box	<b>98.37</b>	<b>97.24</b>

image-text alignment training, EarthMarker is endowed with excellent holistic scene understanding ability on RS imagery.

### C. Image Captioning

To evaluate the image captioning capabilities, we use the NWPU-Captions [41] dataset to assess and compare EarthMarker against other expert models in the supervised setting. Created by Northwestern Polytechnical University, the NWPU-Captions dataset includes 31,500 aerial images and 157,500 sentences for RS image description. Following the protocol of MLCA-Net, we employ BLEU1, BLEU2, BLEU3, BLEU4, METEOR, ROUGE-L, and CIDErD as evaluation metrics. In the evaluation, we use the sentence “Please provide a brief caption of each marked region in the image.” as text instruction and a full-image box  $[0, 0, \text{width}, \text{height}]$  as the visual prompt. As shown in Tab. III, compared to other expert models, EarthMarker demonstrates improvements in BLEU1, BLEU2, BLEU3, BLEU4, METEOR, and ROUGE-L by 7.4%, 8.2%, 8.8%, 6.5%, 3.5%, and 9.9%, respectively, and a 36.5% improvement in CIDErD. In summary, we dexterously annotate the entire image as a single region, and further using both natural and RS image training, EarthMarker achieves a high

level of understanding of the overall image, outperforming expert models.

### D. Referring Object Classification

The referring object classification task aims to identify the category within the referring region in the image. The metrics used to evaluate this task are two semantic relevance indicators—Semantic Similarity (SS) and Semantic Intersection over Union (S-IOU) to assess a model’s classification ability. Closed-set testing is adopted on the test sets of object-level dataset DIOR-RSVG [19]. The text instruction is “Please identify the category of the marked region in the image”, which along with the bounding boxes are fed into LLM to predict the category of regions. Due to the former MLLM (e.g., GeoChat, Sphinx, and EarthGPT) only accepting images and text as input, the region prompt for those MLLMs are coordinates information contained in the text instructions.

As the results shown in Tab. V, EarthMarker achieves 95.96% in SS and 93.49% in S-IoU using point-level visual prompts, and 98.37% in SS and 97.24% in S-IoU based on box-level visual prompts on the DIOR-RSVG dataset. Both sets of results significantly outperform the SOTA method. Furthermore, EarthMarker surpasses the previous SOTA model EarthGPT by 3.73% in SS and 7.08% in S-IoU on the DIOR-RSVG dataset, demonstrating its superior capability in fine-grained box-level classification and the effectiveness of our designed visual prompting method. Additionally, in Fig. 3, there are considerable differences in predictions of regional object categories by EarthMarker and other MLLMs, as well as visual prompting models. It is evident that when faced with complex geographical scenes and blurry tiny objects, EarthMarker’s predictions are significantly accurate.

### E. Region Captioning

For the brief region captioning, the test set of DIOR-RSVG [19] is employed. Specifically, we adopt boxes as the visual prompt and a text prompt, such as “Please provide a

User: Please provide a *brief caption* of each marked region in the image.



<b>EarthMarker (Ours)</b> <Region 1>: A stadium in the middle. <Region 2>: A groundtrackfield on the right. <Region 3>: A tiny tennis court.	<b>Vip-LLava-13B</b> <Region 1>: A large grassy field. <Region 2>: A green field with a white stripe in the middle. <Region 3>: A patch of green grass.
<b>GeoChat</b> <Region 1>: A stadium. <Region 2>: A groundtrackfield at the right. <Region 3>: Some trees at the center.	<b>GLaMM</b> <Region 1>: A large field in the middle of the city. <Region 2>: A large field of grass. <Region 3>: A white line on the field.
<b>EarthGPT</b> <Region 1>: The stadium has the oval ground track field. <Region 2>: The large stadium. <Region 3>: The large stadium.	<b>Sphinx</b> <Region 1>: A ground track field in the middle. <Region 2>: A baseball field in the middle. <Region 3>: A tennis court on the right.

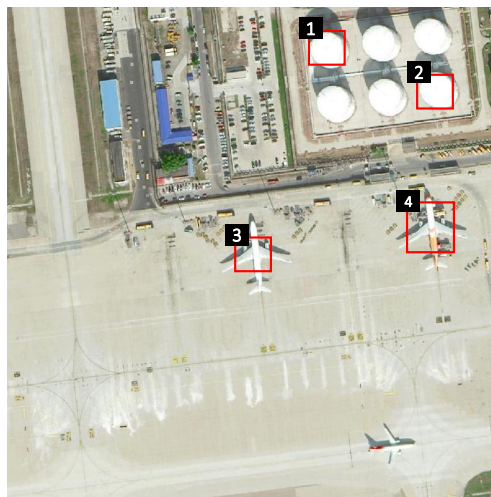
---



<b>EarthMarker (Ours)</b> <Region 1>: A overpass in the middle. <Region 2>: A expressway toll station.	<b>Vip-LLava-13B</b> <Region 1>: A road in the middle of a field. <Region 2>: A patch of dirt with no grass.
<b>GeoChat</b> <Region 1>: A bridge at the center. <Region 2>: Some buildings at the top left.	<b>GLaMM</b> <Region 1>: A road in the photo. <Region 2>: A red and white sign.
<b>EarthGPT</b> <Region 1>: A overpass in the image. <Region 2>: The gray airport.	<b>Sphinx</b> <Region 1>: A gray bridge. <Region 2>: A gray bridge.

Fig. 4. The brief region captioning results on RS images demonstrate the precise fine-grained object-level RS visual comprehension ability of EarthMarker, compared to other MLLMs, visual prompting models. (The symbol  $\checkmark$  indicates consistency with the ground truth, the symbol  $\times$  represents all incorrect answers, the yellow highlights denote errors, and the blue text represents relatively correct responses.)

User: Please analyze the relationship between all marked region in the image.



<b>EarthMarker</b> <ul style="list-style-type: none"> <li>&lt;Region 1&gt; &lt;Region 2&gt; &lt;Region 3&gt; &lt;Region 4&gt;: The marked regions represent different elements of an airport environment.</li> <li>&lt;Region 1&gt; and &lt;Region 2&gt; are both storage tanks, likely used for fuel or other liquids, and are similar in shape and size, suggesting they are part of the same system or facility.</li> <li>&lt;Region 3&gt; and &lt;Region 4&gt; are both commercial airplanes, indicating the area is used for aircraft operations. The positioning of the planes and the tanks suggests a functional airport with operational infrastructure for aircraft and fuel services.</li> </ul>	<b>Sphinx-V</b> <Region 1> <Region 2>: Both marks are associated with storage tanks, which are part of the airport's fuel storage facilities. They are positioned in close proximity to each other, suggesting they are within the same area of the airport. The tanks are similar in appearance and likely serve the same function. <Region 3> <Region 4>: These marks are related to aircraft, with <Region 3> showing a parked plane and <Region 4> depicting a plane on the ground. Both are situated on the tarmac, indicating they are part of the airport's operational environment. They differ in orientation and activity state, with <Region 3> stationary and <Region 4> in motion or preparing for departure.
<b>Vip-LLava</b> The objects marked with "1" "2" "3" "4" are airplanes. They are positioned in a line, with each airplane numbered sequentially.	<b>GPT-4V</b> Regions 3 and 4 are directly involved in the movement and management of aircraft. They are likely positioned along the same taxiway path, facilitating the orderly flow of aircraft to and from runways and gates. Region 2 supports these operations by ensuring that fuel is readily available for the aircraft serviced at the airport. Its placement is strategic, likely considering safety regulations that dictate distance from active taxiways and terminals. Region 1 supports all other regions indirectly by housing vehicles and equipment necessary for ground operations, including baggage handling, maintenance, and possibly emergency services.

Fig. 5. Examples of completing complex RS tasks such as key target inter-relationship analyses. (The yellow highlights denote errors.)

brief caption of each marked region in the image.” to prompt EarthMarker to concisely describe the content of the specified region using a brief caption. Similar to the image captioning task, metrics like BLEU1, BLEU2, BLEU3, BLEU4, METEOR, ROUGE-L, and SPICE are used to evaluate EarthMarker and other MLLMs, visual prompting models in region target understanding.

As displayed in Tab. IV, on the DIOR-RSVG test set, compared to other MLLMs such as Qwen-VL-Chat, GeoChat, Sphinx, EarthGPT, and visual prompting models such as Sphinx-V, ViP-LLava, and GLAMM, EarthMarker shows improvements of 7.72%, 9.99%, 11.38%, 12.67%, blue12.49%, 7.92%, 10.97%, 165.67%, and 17.50% in BLEU1, BLEU2, BLEU3, BLEU4, METEOR, ROUGE-L, CIDER and SPICE, respectively. Furthermore, we visualize the instances of EarthMarker and other models on the region captioning task, as shown in Fig. 4. In complex RS scenarios with numerous targets and extensive geographic coverage, EarthMarker can accurately identify and describe various specified targets, which are challenging tasks for other models. For example, compared to the proposed EarthMarker, the current popular MLLMs like GeoChat and EarthGPT are still inferior in regional comprehension. This excellent performance is mainly attributed to the region-text training and the dual instructions design of visual prompts and language.

#### F. Complex Visual Reasoning

In this part, we present the qualitative experimental result of EarthMarker to demonstrate its proficiency in completing complex RS tasks such as key target inter-relationship analyses. The text instruction for the relationship analyses task is “Please analyze the relationship between all marked regions in the image.” As shown in Fig. 5, when faced with an airport scenario, four visual models provided different responses.

Specifically, the response generated by GPT-4V does not specify the exact categories of each marked region. Additionally, GPT4V incorrectly describes Region 1 as “Region 1 supports all other regions indirectly by housing vehicles and equipment necessary for ground operations, including baggage handling, maintenance, and possibly emergency services”, whereas Region 1 actually contains fuel storage tanks. The Vip-LLava model incorrectly identifies all regions as airplanes. Note that Sphinx-V correctly identifies the types of objects in each region and analyzes the internal relationship of some regions. For example, the Sphinx-V answer “They are positioned in close proximity to each other, suggesting they are within the same area of the airport. The tanks are similar in appearance and likely serve the same function.” However, it fails to provide a comprehensive analysis of the relationships among all four regions, and incorrectly states that the airplane in Region 4 is in motion.

In contrast, our EarthMarker delivers an exemplary response. It firstly summarizes the relationship of all marked regions representing different elements of an airport environment. It then analyzes functionally similar areas in detail, stating that “< Region1 > and < Region2 > are both storage tanks, likely used for fuel or other liquids, and are

similar in shape and size, suggesting they are part of the same system or facility. < Region3 > and < Region4 > are both commercial airplanes, indicating the area is used for aircraft operations. The positioning of the planes and the tanks suggests a functional airport with operational infrastructure for aircraft and fuel services.” This response accurately reflects the diverse functionalities within the airport, demonstrating superior comprehension and analysis compared to the other visual prompting MLLMs.

## VI. CONCLUSION

In this paper, the fine-grained MLLM called EarthMarker, the first visual prompting model specifically designed for the RS domain, is proposed. Furthermore, the RS visual prompting instruction dataset called RSVP is constructed for the first time, facilitating the development of fine-grained RS imagery comprehension. In addition, the visual prompts learning framework is developed. Particularly, the shared visual encoding method is developed to uniformly refine multi-scale visual features and visual prompt content, which is beneficial for comprehensively understanding the interplay between visual prompts and the holistic image. Subsequently, the referring areas in the input are replaced by the proposed hybrid representation before being fed into the LLM to instruct the model to comprehend referring areas and toward specific predictions. Employing the RSVP-3M and the visual prompt learning framework, EarthMarker is equipped with multi-granularity visual understanding capability at the image, region, and point levels, making it able to simultaneously perform comprehensive and intelligent analysis in real-world scenarios. In the future, we plan to incorporate a broader range of visual modalities into EarthMarker, enhancing its multi-source imagery comprehension capabilities. In addition, we plan to support free-form shapes as visual marks to adjust the referring granularity flexibly.

## REFERENCES

- [1] Amir Bar, Yossi Gandelsman, Trevor Darrell, Amir Globerson, and Alexei Efros. Visual prompting via image inpainting. *Advances in Neural Information Processing Systems*, 35:25005–25017, 2022.
- [2] Liang Zhao, En Yu, Zheng Ge, Jinrong Yang, Haoran Wei, Hongyu Zhou, Jianjian Sun, Yuang Peng, Runpei Dong, Chunrui Han, et al. Chatspot: Bootstrapping multimodal llms via precise referring instruction tuning. *arXiv preprint arXiv:2307.09474*, 2023.
- [3] Razieh Rezaei, Masoud Jalili Sabet, Jindong Gu, Daniel Rueckert, Philip Torr, and Ashkan Khakzar. Learning visual prompts for guiding the attention of vision transformers. *arXiv preprint arXiv:2406.03303*, 2024.
- [4] Kartik Kuckreja, Muhammad Sohail Danish, Muzammal Naseer, Abhijit Das, Salman Khan, and Fahad Shahbaz Khan. Geochat: Grounded large vision-language model for remote sensing. *arXiv preprint arXiv:2311.15826*, 2023.
- [5] Wei Zhang, Miaoxin Cai, Tong Zhang, Yin Zhuang, and Xuerui Mao. Earthgpt: A universal multi-modal large language model for multi-sensor image comprehension in remote sensing domain. *IEEE Transactions on Geoscience and Remote Sensing*, 2024.
- [6] Xiao Xiang Zhu, Devis Tuia, Lichao Mou, Gui-Song Xia, Liangpei Zhang, Feng Xu, and Friedrich Fraundorfer. Deep learning in remote sensing: A comprehensive review and list of resources. *IEEE Geoscience and Remote Sensing Magazine*, 5(4):8–36, 2017.
- [7] Taylor Shin, Yasaman Razeghi, Robert L Logan IV, Eric Wallace, and Sameer Singh. Autoprompt: Eliciting knowledge from language models with automatically generated prompts. *arXiv preprint arXiv:2010.15980*, 2020.

- [8] Kaiyang Zhou, Jingkang Yang, Chen Change Loy, and Ziwei Liu. Learning to prompt for vision-language models. *International Journal of Computer Vision*, 130(9):2337–2348, 2022.
- [9] Pengfei Liu, Weizhe Yuan, Jinlan Fu, Zhengbao Jiang, Hiroaki Hayashi, and Graham Neubig. Pre-train, prompt, and predict: A systematic survey of prompting methods in natural language processing. *ACM Computing Surveys*, 55(9):1–35, 2023.
- [10] Alexander Kirillov, Eric Mintun, Nikhila Ravi, Hanzi Mao, Chloe Rolland, Laura Gustafson, Tete Xiao, Spencer Whitehead, Alexander C Berg, Wan-Yen Lo, et al. Segment anything. In *Proceedings of the IEEE/CVF International Conference on Computer Vision*, pages 4015–4026, 2023.
- [11] Shilong Zhang, Peize Sun, Shoufa Chen, Min Xiao, Wenqi Shao, Wenwei Zhang, Kai Chen, and Ping Luo. Gpt4roi: Instruction tuning large language model on region-of-interest. *arXiv preprint arXiv:2307.03601*, 2023.
- [12] Qiang Zhou, Chaohui Yu, Shaofeng Zhang, Sitong Wu, Zhibing Wang, and Fan Wang. Regionblip: A unified multi-modal pre-training framework for holistic and regional comprehension. *arXiv preprint arXiv:2308.02299*, 2023.
- [13] Yuqian Yuan, Wentong Li, Jian Liu, Dongqi Tang, Xinjie Luo, Chi Qin, Lei Zhang, and Jianke Zhu. Osprey: Pixel understanding with visual instruction tuning. *arXiv preprint arXiv:2312.10032*, 2023.
- [14] Haoxuan You, Haotian Zhang, Zhe Gan, Xianzhi Du, Bowen Zhang, Zirui Wang, Liangliang Cao, Shih-Fu Chang, and Yinfei Yang. Ferret: Refer and ground anything anywhere at any granularity. *arXiv preprint arXiv:2310.07704*, 2023.
- [15] Weifeng Lin, Xinyu Wei, Ruichuan An, Peng Gao, Bocheng Zou, Yulin Luo, Siyuan Huang, Shanghang Zhang, and Hongsheng Li. Draw-and-understand: Leveraging visual prompts to enable mllms to comprehend what you want. *arXiv preprint arXiv:2403.20271*, 2024.
- [16] Yang Zhan, Zhitong Xiong, and Yuan Yuan. Rsvg: Exploring data and models for visual grounding on remote sensing data. *IEEE Transactions on Geoscience and Remote Sensing*, 61:1–13, 2023.
- [17] Keyan Chen, Chenyang Liu, Hao Chen, Haotian Zhang, Wenyuan Li, Zhengxia Zou, and Zhenwei Shi. Rsprompter: Learning to prompt for remote sensing instance segmentation based on visual foundation model. *IEEE Transactions on Geoscience and Remote Sensing*, 2024.
- [18] Josh Achiam, Steven Adler, Sandhini Agarwal, Lama Ahmad, Ilge Akkaya, Florencia Leoni Aleman, Diogo Almeida, Janko Altmenschmidt, Sam Altman, Shyamal Anadkat, et al. Gpt-4 technical report. *arXiv preprint arXiv:2303.08774*, 2023.
- [19] Yang Zhan, Zhitong Xiong, and Yuan Yuan. Rsvg: Exploring data and models for visual grounding on remote sensing data. *IEEE Transactions on Geoscience and Remote Sensing*, 61:1–13, 2023.
- [20] Tom Brown, Benjamin Mann, Nick Ryder, Melanie Subbiah, Jared D Kaplan, Prafulla Dhariwal, Arvind Neelakantan, Pranav Shyam, Girish Sastry, Amanda Askell, et al. Language models are few-shot learners. *Advances in neural information processing systems*, 33:1877–1901, 2020.
- [21] Hugo Touvron, Thibaut Lavril, Gautier Izacard, Xavier Martinet, Marie-Anne Lachaux, Timothée Lacroix, Baptiste Rozière, Naman Goyal, Eric Hambro, Faisal Azhar, et al. Llama: Open and efficient foundation language models. *arXiv preprint arXiv:2302.13971*, 2023a.
- [22] Hugo Touvron, Louis Martin, Kevin Stone, Peter Albert, Amjad Almahairi, Yasmine Babaei, Nikolay Bashlykov, Soumya Batra, Prajjwal Bhargava, Shruiti Bhosale, et al. Llama 2: Open foundation and fine-tuned chat models. *arXiv preprint arXiv:2307.09288*, 2023b.
- [23] Jun Chen, Han Guo, Kai Yi, Boyang Li, and Mohamed Elhoseiny. Visualgpt: Data-efficient adaptation of pretrained language models for image captioning. In *Proceedings of the IEEE/CVF Conference on Computer Vision and Pattern Recognition*, pages 18030–18040, 2022.
- [24] Junnan Li, Dongxu Li, Silvio Savarese, and Steven Hoi. Blip-2: Bootstrapping language-image pre-training with frozen image encoders and large language models. *arXiv preprint arXiv:2301.12597*, 2023.
- [25] Jean-Baptiste Alayrac, Jeff Donahue, Pauline Luc, Antoine Miech, Iain Barr, Yana Hasson, Karel Lenc, Arthur Mensch, Katherine Millican, Malcolm Reynolds, et al. Flamingo: A visual language model for few-shot learning. *Advances in Neural Information Processing Systems*, 35:23716–23736, 2022.
- [26] Peng Gao, Jiaming Han, Renrui Zhang, Ziyi Lin, Shijie Geng, Aojun Zhou, Wei Zhang, Pan Lu, Conghui He, Xiangyu Yue, et al. Llama-adapter v2: Parameter-efficient visual instruction model. *arXiv preprint arXiv:2304.15010*, 2023.
- [27] Ziyi Lin, Chris Liu, Renrui Zhang, Peng Gao, Longtian Qiu, Han Xiao, Han Qiu, Chen Lin, Wenqi Shao, Keqin Chen, et al. Sphinx: The joint mixing of weights, tasks, and visual embeddings for multi-modal large language models. *arXiv preprint arXiv:2311.07575*, 2023.
- [28] Yang Zhan, Zhitong Xiong, and Yuan Yuan. Skyeegpt: Unifying remote sensing vision-language tasks via instruction tuning with large language model. *arXiv preprint arXiv:2401.09712*, 2024.
- [29] Yu Du, Fangyun Wei, Ziheng Zhang, Miaojing Shi, Yue Gao, and Guoqi Li. Learning to prompt for open-vocabulary object detection with vision-language model. In *Proceedings of the IEEE/CVF Conference on Computer Vision and Pattern Recognition*, pages 14084–14093, 2022.
- [30] Chengjian Feng, Yujie Zhong, Zequn Jie, Xiangxiang Chu, Haibing Ren, Xiaolin Wei, Weidi Xie, and Lin Ma. Promptdet: Towards open-vocabulary detection using uncurated images. In *European Conference on Computer Vision*, pages 701–717. Springer, 2022.
- [31] Feng Li, Hao Zhang, Peize Sun, Xueyan Zou, Shilong Liu, Jianwei Yang, Chunyuan Li, Lei Zhang, and Jianfeng Gao. Semantic-sam: Segment and recognize anything at any granularity. *arXiv preprint arXiv:2307.04767*, 2023.
- [32] Yuan Yao, Ao Zhang, Zhengyan Zhang, Zhiyuan Liu, Tat-Seng Chua, and Maosong Sun. Cpt: Colorful prompt tuning for pre-trained vision-language models, 2022.
- [33] Zhiliang Peng, Wenhui Wang, Li Dong, Yaru Hao, Shaohan Huang, Shuming Ma, and Furu Wei. Kosmos-2: Grounding multimodal large language models to the world. *arXiv preprint arXiv:2306.14824*, 2023.
- [34] Keqin Chen, Zhao Zhang, Weili Zeng, Richong Zhang, Feng Zhu, and Rui Zhao. Shikra: Unleashing multimodal llm’s referential dialogue magic. *arXiv preprint arXiv:2306.15195*, 2023.
- [35] Peng Gao, Renrui Zhang, Chris Liu, Longtian Qiu, Siyuan Huang, Weifeng Lin, Shitian Zhao, Shijie Geng, Ziyi Lin, Peng Jin, et al. Sphinx-x: Scaling data and parameters for a family of multi-modal large language models. *arXiv preprint arXiv:2402.05935*, 2024.
- [36] Maxime Oquab, Timothée Darcet, Théo Moutakanni, Huy Vo, Marc Szafraniec, Vasil Khalidov, Pierre Fernandez, Daniel Haziza, Francisco Massa, Alaaeldin El-Nouby, et al. Dinov2: Learning robust visual features without supervision. *arXiv preprint arXiv:2304.07193*, 2023.
- [37] Alec Radford, Jong Wook Kim, Chris Hallacy, Aditya Ramesh, Gabriel Goh, Sandhini Agarwal, Girish Sastry, Amanda Askell, Pamela Mishkin, Jack Clark, et al. Learning transferable visual models from natural language supervision. In *International conference on machine learning*, pages 8748–8763. PMLR, 2021.
- [38] Xinlei Chen, Hao Fang, Tsung-Yi Lin, Ramakrishna Vedantam, Saurabh Gupta, Piotr Dollár, and C Lawrence Zitnick. Microsoft coco captions: Data collection and evaluation server. *arXiv preprint arXiv:1504.00325*, 2015.
- [39] Sahar Kazemzadeh, Vicente Ordonez, Mark Matten, and Tamara Berg. Referitgame: Referring to objects in photographs of natural scenes. In *Proceedings of the 2014 conference on empirical methods in natural language processing (EMNLP)*, pages 787–798, 2014.
- [40] Licheng Yu, Patrick Poirson, Shan Yang, Alexander C. Berg, and Tamara L. Berg. Modeling context in referring expressions, 2016.
- [41] Qimin Cheng, Haiyan Huang, Yuan Xu, Yuzhuo Zhou, Huanying Li, and Zhongyuan Wang. Nwpu-captions dataset and mlca-net for remote sensing image captioning. *IEEE Transactions on Geoscience and Remote Sensing*, 60:1–19, 2022.
- [42] Zhiqiang Yuan, Wenkai Zhang, Kun Fu, Xuan Li, Chubo Deng, Hongqi Wang, and Xian Sun. Exploring a fine-grained multiscale method for cross-modal remote sensing image retrieval. *arXiv preprint arXiv:2204.09868*, 2022.
- [43] Bo Qu, Xuelong Li, Dacheng Tao, and Xiaoqiang Lu. Deep semantic understanding of high resolution remote sensing image. In *2016 International conference on computer, information and telecommunication systems (Cits)*, pages 1–5. IEEE, 2016.
- [44] Gong Cheng, Junwei Han, and Xiaoqiang Lu. Remote sensing image scene classification: Benchmark and state of the art. *Proceedings of the IEEE*, 105(10):1865–1883, 2017.
- [45] Qi Wang, Shaoteng Liu, Jocelyn Chanut, and Xuelong Li. Scene classification with recurrent attention of vhr remote sensing images. *IEEE Transactions on Geoscience and Remote Sensing*, 57(2):1155–1167, 2018.
- [46] Yang Long, Yiping Gong, Zhifeng Xiao, and Qing Liu. Accurate object localization in remote sensing images based on convolutional neural networks. *IEEE Transactions on Geoscience and Remote Sensing*, 55(5):2486–2498, 2017.
- [47] Dengxin Dai and Wen Yang. Satellite image classification via two-layer sparse coding with biased image representation. *IEEE Geoscience and remote sensing letters*, 8(1):173–176, 2010.
- [48] Jian Ding, Nan Xue, Gui-Song Xia, Xiang Bai, Wen Yang, Michael Yang, Serge Belongie, Jiebo Luo, Mihai Datcu, Marcello Pelillo, and

- Liangpei Zhang. Object detection in aerial images: A large-scale benchmark and challenges. *IEEE Transactions on Pattern Analysis and Machine Intelligence*, pages 1–1, 2021.
- [49] Xian Sun, Peijin Wang, Zhiyuan Yan, Feng Xu, Ruiping Wang, Wenhui Diao, Jin Chen, Jihao Li, Yingchao Feng, Tao Xu, et al. Fair1m: A benchmark dataset for fine-grained object recognition in high-resolution remote sensing imagery. *ISPRS Journal of Photogrammetry and Remote Sensing*, 184:116–130, 2022.
- [50] Gong Cheng, Peicheng Zhou, and Junwei Han. Learning rotation-invariant convolutional neural networks for object detection in vhr optical remote sensing images. *IEEE transactions on geoscience and remote sensing*, 54(12):7405–7415, 2016.
- [51] Haigang Zhu, Xiaogang Chen, Weiqun Dai, Kun Fu, Qixiang Ye, and Jianbin Jiao. Orientation robust object detection in aerial images using deep convolutional neural network. In *2015 IEEE International Conference on Image Processing (ICIP)*, pages 3735–3739. IEEE, 2015.
- [52] Pengfei Zhu, Longyin Wen, Dawei Du, Xiao Bian, Heng Fan, Qinghua Hu, and Haibin Ling. Detection and tracking meet drones challenge. *IEEE Transactions on Pattern Analysis and Machine Intelligence*, 44(11):7380–7399, 2021.
- [53] YU Wenqi, CHENG Gong, WANG Meijun, YAO Yanqing, XIE Xingxing, YAO Xiwen, and HAN Junwei. Mar20: A benchmark for military aircraft recognition in remote sensing images. *National Remote Sensing Bulletin*, 27(12):2688–2696, 2024.
- [54] Yaqi Han, Xinyi Yang, Tian Pu, and Zhenming Peng. Fine-grained recognition for oriented ship against complex scenes in optical remote sensing images. *IEEE Transactions on Geoscience and Remote Sensing*, 60:1–18, 2021.
- [55] Zhengxia Zou and Zhenwei Shi. Random access memories: A new paradigm for target detection in high resolution aerial remote sensing images. *IEEE Transactions on Image Processing*, 27(3):1100–1111, 2017.
- [56] Zikun Liu, Liu Yuan, Lubin Weng, and Yiping Yang. A high resolution optical satellite image dataset for ship recognition and some new baselines. In *International conference on pattern recognition applications and methods*, volume 2, pages 324–331. SciTePress, 2017.
- [57] Yuanlin Zhang, Yuan Yuan, Yachuang Feng, and Xiaoqiang Lu. Hierarchical and robust convolutional neural network for very high-resolution remote sensing object detection. *IEEE Transactions on Geoscience and Remote Sensing*, 57(8):5535–5548, 2019.
- [58] isprs. Urban modelling and semantic labelling benchmark. <https://www.isprs.org/education/benchmarks/UrbanSemLab/Default.aspx/>, 2021.
- [59] Shiqi Tian, Ailong Ma, Zhuo Zheng, and Yanfei Zhong. Hi-ucd: A large-scale dataset for urban semantic change detection in remote sensing imagery. *arXiv preprint arXiv:2011.03247*, 2020.
- [60] Syed Waqas Zamir, Aditya Arora, Akshita Gupta, Salman Khan, Guolei Sun, Fahad Shahbaz Khan, Fan Zhu, Ling Shao, Gui-Song Xia, and Xiang Bai. isaid: A large-scale dataset for instance segmentation in aerial images. In *Proceedings of the IEEE Conference on Computer Vision and Pattern Recognition Workshops*, pages 28–37, 2019.
- [61] Ye Lyu, George Vosselman, Gui-Song Xia, Alper Yilmaz, and Michael Ying Yang. Uavid: A semantic segmentation dataset for uav imagery. *ISPRS Journal of Photogrammetry and Remote Sensing*, 165:108 – 119, 2020.
- [62] Di Wang, Jing Zhang, Bo Du, Minqiang Xu, Lin Liu, Dacheng Tao, and Liangpei Zhang. Samrs: Scaling-up remote sensing segmentation dataset with segment anything model. *Advances in Neural Information Processing Systems*, 36, 2024.
- [63] Shunping Ji, Shiqing Wei, and Meng Lu. Fully convolutional networks for multisource building extraction from an open aerial and satellite imagery data set. *IEEE Transactions on geoscience and remote sensing*, 57(1):574–586, 2018.
- [64] Jianwei Yang et al. Set-of-mark prompting unleashes extraordinary visual grounding in gpt-4v. *arXiv preprint arXiv:2310.11441*, 2023.
- [65] Diederik P Kingma and Jimmy Ba. Adam: A method for stochastic optimization. *arXiv preprint arXiv:1412.6980*, 2014.
- [66] Jinze Bai, Shuai Bai, Shusheng Yang, Shijie Wang, Sinan Tan, Peng Wang, Junyang Lin, Chang Zhou, and Jingren Zhou. Qwen-vl: A frontier large vision-language model with versatile abilities. *arXiv preprint arXiv:2308.12966*, 2023.
- [67] Jun Chen, Deyao Zhu, Xiaoqian Shen, Xiang Li, Zechun Liu, Pengchuan Zhang, Raghuraman Krishnamoorthi, Vikas Chandra, Yunyang Xiong, and Mohamed Elhoseiny. Minigpt-v2: large language model as a unified interface for vision-language multi-task learning. *arXiv preprint arXiv:2310.09478*, 2023.
- [68] Haotian Liu, Chunyuan Li, Qingyang Wu, and Yong Jae Lee. Visual instruction tuning. *arXiv preprint arXiv:2304.08485*, 2023.
- [69] Kartik Kuckreja, Muhammad Sohail Danish, Muzammal Naseer, Abhijit Das, Salman Khan, and Fahad Shahbaz Khan. Geochat: Grounded large vision-language model for remote sensing. In *Proceedings of the IEEE/CVF Conference on Computer Vision and Pattern Recognition*, pages 27831–27840, 2024.
- [70] Binqiang Wang, Xiaoqiang Lu, Xiangtao Zheng, and Xuelong Li. Semantic descriptions of high-resolution remote sensing images. *IEEE Geoscience and Remote Sensing Letters*, 16(8):1274–1278, 2019.
- [71] Xiaoqiang Lu, Binqiang Wang, Xiangtao Zheng, and Xuelong Li. Exploring models and data for remote sensing image caption generation. *IEEE Transactions on Geoscience and Remote Sensing*, 56(4):2183–2195, 2017.
- [72] Xiangrong Zhang, Xin Wang, Xu Tang, Huiyu Zhou, and Chen Li. Description generation for remote sensing images using attribute attention mechanism. *Remote Sensing*, 11(6):612, 2019.
- [73] Qimin Cheng, Haiyan Huang, Yuan Xu, Yuzhuo Zhou, Huanying Li, and Zhongyuan Wang. Nwpu-captions dataset and mlca-net for remote sensing image captioning. *IEEE Transactions on Geoscience and Remote Sensing*, 60:1–19, 2022.
- [74] Gui-Song Xia, Jingwen Hu, Fan Hu, Baoguang Shi, Xiang Bai, Yanfei Zhong, Liangpei Zhang, and Xiaoqiang Lu. Aid: A benchmark data set for performance evaluation of aerial scene classification. *IEEE Transactions on Geoscience and Remote Sensing*, 55(7):3965–3981, 2017.
- [75] Yi Yang and Shawn Newsam. Bag-of-visual-words and spatial extensions for land-use classification. In *Proceedings of the 18th SIGSPATIAL international conference on advances in geographic information systems*, pages 270–279, 2010.
- [76] Mu Cai, Haotian Liu, Siva Karthik Mustikovela, Gregory P Meyer, Yuning Chai, Dennis Park, and Yong Jae Lee. Vip-llava: Making large multimodal models understand arbitrary visual prompts. In *Proceedings of the IEEE/CVF Conference on Computer Vision and Pattern Recognition*, pages 12914–12923, 2024.